WAVE PROPAGATION IN THE EFFECTIVE MODEL OF ALTERNATING POROUS AND IMPERMEABLE SOLID LAYERS

L. MOLOTKOV

Russian Academy of Sciences[1]

A. BAKULIN

Saint-Petersburg State University[2]

PROPAGATION DES ONDES DANS UN MODÈLE EFFECTIF CONSTITUÉ DE COUCHES SOLIDES ALTERNATIVEMENT POREUSES ET IMPERMÉABLES

Les propriétés élastiques des milieux finement stratifiés présentent un grand intérêt pour l'exploration sismique. Les modèles théoriques donnent les propriétés générales en fonction des paramètres des constituants. D'une part, ils aident les géophysiciens à évaluer les gammes d'anisotropie possibles, et d'autre part, ils offrent une base pour l'interprétation des paramètres d'anisotropie mesurés en termes de microstructure. De tels modèles, élastiques, ont été largement utilisés ces quarante dernières années. Ils ont été récemment remis à jour pour la description des roches fracturées (Hsu et Schoenberg, 1993). Dans ce cas, il s'agit de modèles stratifiés élastiques à fractures. Toutefois, les roches-réservoirs sont poreuses et perméables. La porosité et la perméabilité sont prises en compte dans le modèle bien connu de Biot. Les séquences poreuses finement stratifiées ont certaines propriétés distinctes qui font l'objet de recherches actuelles (Schoenberg, 1996). Il est donc devenu important de remettre à jour les concepts développés sur les milieux poreux. Bakulin et Molotkov (1998, 1997) ont effectué la première étape en généralisant aux milieux poroélastiques la technique d'homogénéisation de Backus . Nous nous concentrons ici sur un cas particulier où il n'y a qu'une direction préférentielle de l'écoulement du fluide dans les roches poreuses. Ceci peut être provoqué par la présence de barrières imperméables ou de formes lenticulaires, qui sont modélisées comme un ensemble de couches solides croisant des milieux poreux. Un tel modèle correspond à des roches fortement anisotropes vis-à-vis des propriétés hydrauliques, et présente une très forte anisotropie de structure de son espace poreux.

WAVE PROPAGATION IN THE EFFECTIVE MODEL OF ALTERNATING POROUS AND IMPERMEABLE SOLID LAYERS

Elastic properties of finely layered media are of great interest for seismic exploration. Theoretical models give a dependence of overall properties on constituent parameters. On the one hand they help geophysicists to estimate possible ranges of anisotropy and on the other hand they provide a basis for interpretation of measured anisotropic parameters in terms of microstructure. Last forty years such models with elastic constituents have been extensively used. Recently they have been updated for describing fractured rocks (Hsu and Schoenberg, 1993). In this case thin, and

(1) Saint-Petersburg Branch of Steklov Mathematical Institut, Saint-Petersburg - Russia
(2) Geological Faculty, Department of Geophysics, Saint-Petersburg - Russia

soft elastic layer models fracture. However reservoir rocks are porous and permeable. Porosity and permeability are taken into account by well-known Biot model. Finely layered porous sequences have some distinctive properties which are the topic of modern research (Schoenberg, 1996). Therefore it is important to update developed concepts to porous medium. Bakulin and Molotkov (1998, 1997) who generalized Backus averaging on poroelastic medium have done first step. Here we pay attention to one special case when there is only one preferential direction of fluid flow in porous rock. This may be caused by presence of impermeable barriers or lenses, which are modeled as set of solid layers intersecting porous medium. Such model corresponds to highly hydraulically anisotropic rock, which has very strong anisotropy of pore space structure and permeability.

PROPAGACIÓN DE ONDAS EN EL MODELO EFECTIVO DE ALTERNANCIA DE CAPAS SÓLIDAS POROSAS Y IMPERMEABLES

Las propiedades de medios finamente estratificados son de gran importancia en la exploración sísmica. Los modelos teóricos proporcionan una dependencia de las propiedades globales con respecto a los parámetros constitutivos. Por una parte, ayudan a los geofísicos a estimar posibles rangos de anisotropía y, por otra, proporcionan una base para interpretar parámetros anisotrópicos medidos en términos de microestructura. En los últimos cuarenta años han sido ampliamente utilizados estos modelos con constituyentes elásticos. Han sido actualizados recientemente para describir rocas fracturadas (Hsu y Schoenberg, 1993). En este caso, fracturas en modelos de capas clásticas delgadas y blandas. Sin embargo, las rocas de los depósitos son porosas y permeables. La porosidad y la permeabilidad son tomadas en cuenta en un modelo Biot, ampliamente conocido. Las secuencias porosas finamente estratificadas tienen ciertas propiedades características que constituyen el objeto de investigaciones modernas (Schoenberg, 1996). Por lo tanto, resulta importante actualizar los conceptos desarrollados incluyendo medios porosos. Bakulin y Molotkov (1998, 1997), al generalizar los promedios Backus en el medio poroelástico, han dado un primer paso en este sentido. En este artículo prestamos atención a un caso especial: el que se presenta cuando existe una sola dirección preferencial de flujo del fluido dentro de la roca porosa. Esto puede ser causado por la presencia de barreras o lentes impermeables, modelados como un conjunto de capas sólidas que intersectan el medio poroso. Dicho modelo corresponde a una roca muy hidráulicamente isotrópica, que tiene una fuerte anisotropía en la estructura y permeabilidad del espacio poroso.

INTRODUCTION

The effective model of alternating porous and solid layers was derived by the method of matrix averaging (Bakulin and Molotkov, 1998; Molotkov and Bakulin, 1997a, 1997b). This model is a special case of the transversely isotropic Biot model. Purpose of this paper is to derive the expressions for the velocities along the axes, to construct wave fronts from a point source and to reveal some new features of these fronts. For obtaining wave fronts we use the approach suggested by Molotkov and Khilo (1984). Points of the fronts are defined by parametric formulas in terms of the characteristic functions which are solutions of Christoffel Equation. Parametric formulas are the conditions determining the location of the singularities of the integral representation of wave field. This approach is similar to the method, which uses slowness surfaces for constructing wave fronts (Fedorov, 1968; Musgrave, 1970; Helbig, 1994).

The difference between these two methods is in choice of characteristic functions. Due to the successful choice the characteristic functions become the solutions of biquadratic equation. Therefore these functions may be analytically analyzed as well as parametric formulas for the front. First of all we discuss the wave fronts in the case, when they have no loops. In this case there are minimum number of points of inflection and there are no turning points on the graphs of the characteristic functions. Then we consider the cases when on the mentioned graphs there are turning points and additional points of inflection. In these cases second and third fronts may have a loops on the axes or between axes.

The complication of the fronts is restricted by the condition that an arbitrary straight line could intersect the graphs of characteristic function no more than at six points. The analogous restriction was established for intersections with slowness surfaces.

1 THE EFFECTIVE MODEL

We consider stratified periodic medium of alternating porous Biot layers 1 and impermeable solid layers 2 (Fig. 1). On internal interfaces of this medium the relative normal displacement of the fluid phase vanishes whereas skeleton of porous layer and material of elastic layer are in welded contact.
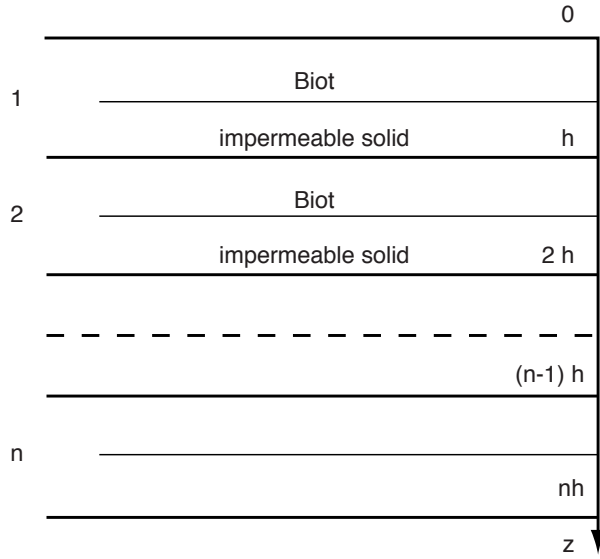
Figure 1

Stack of porous Biot and impermeable solid layers.

The effective model of this medium is described by Equations (Molotkov and Bakulin, 1997a, 1997b; Bakulin and Molotkov, 1998) (1.1) and (1.2) where U_x, U_z, and $\tau_{xx}, \tau_{xz}, \tau_{zz}$ are displacements in the solid phase and total bulk stresses respectively, W_x and p are relative displacement and pressure in the fluid phase, is averaged density of the medium, and f is density of the fluid phase.

The coefficients in Equations (1.1) and (1.2) are defined by expression (1.3) and (1.4).

In formulas (1.3) and (1.4), Θ_1 and Θ_2 are relative parts of the volume occupied by porous and solid layers respectively ($\Theta_1 + \Theta_2 = 1$).

Porous layer is determined by elastic moduli $\tilde{P}, \tilde{F}, \tilde{M}, \tilde{C}, \tilde{Q}, \tilde{R}, \tilde{L}$, averaged bulk density $\bar{\rho}$ and density of the fluid phase $\tilde{\rho}_f$.

Density $\tilde{m}_x$ is defined as $\tilde{m}_x = \tilde{\rho}_f \tilde{\alpha}/\varepsilon$ where $\tilde{\alpha}$ is a dimensionless tortuosity of pore space and ε is porosity. Parameter $\tilde{b}_x = \tilde{\eta}/\tilde{\kappa}_x$ depends on fluid viscosity $\tilde{\eta}$ and horizontal permeability $\tilde{\kappa}_x$ of the porous layer.

$$\tau_{xx} = P\frac{\partial U_x}{\partial x} + F\frac{\partial U_z}{\partial z} + M\frac{\partial W_x}{\partial x} \quad \tau_{zz} = F\frac{\partial U_x}{\partial x} + C\frac{\partial U_z}{\partial z} + Q\frac{\partial W_x}{\partial x}$$

$$-p = M\frac{\partial U_x}{\partial x} + Q\frac{\partial U_z}{\partial z} + R\frac{\partial W_x}{\partial x} \quad \tau_{xz} = L\left(\frac{\partial U_x}{\partial z} + F\frac{\partial U_z}{\partial x}\right)$$

(1.1)

$$\frac{\partial \tau_{xx}}{\partial x} + \frac{\partial \tau_{xz}}{\partial z} = r\frac{\partial^2 U_x}{\partial t^2} + r_f\frac{\partial^2 W_x}{\partial t^2} \quad -\frac{\partial p}{\partial x} = r_f\frac{\partial^2 U_x}{\partial t^2} + m_x\frac{\partial^2 W_x}{\partial t^2} + b_x\frac{\partial W_x}{\partial t}$$

$$\frac{\partial \tau_{xz}}{\partial x} + \frac{\partial \tau_{zz}}{\partial z} = r\frac{\partial^2 U_z}{\partial t^2}$$

(1.2)

$$P = A_3 + A_1\tilde{F} - A_2\tilde{M} \quad F = \frac{A_1 A_5 - A_2 A_4}{A_5 A_6 - A_4^2} \quad M = \frac{A_1 A_4 - A_2 A_6}{A_5 A_6 - A_4^2} \quad C = \frac{A_5}{A_5 A_6 - A_4^2}$$

$$R = \frac{A_6}{A_5 A_6 - A_4^2} \quad L = \frac{1}{A_7} \quad \rho = \bar{\rho}\Theta_1 + \tilde{\rho}\Theta_2 \quad \rho_f = \tilde{\rho}_f \quad m_x = \frac{\tilde{m}_x}{\Theta_1} \quad b_x = \frac{\tilde{b}_x}{\Theta_1}$$

(1.3)

$$A_1 = \frac{\tilde{F}\tilde{R} - \tilde{M}\tilde{Q}}{\tilde{C}\tilde{R} - \tilde{Q}^2}\Theta_1 + \frac{\lambda\Theta_2}{\lambda + 2\mu} \quad A_2 = \frac{\tilde{F}\tilde{Q} - \tilde{C}\tilde{M}}{\tilde{C}\tilde{R} - \tilde{Q}^2}\Theta_1 \quad A_3 = \frac{\Delta\Theta_1}{\tilde{C}\tilde{R} - \tilde{Q}^2} + \frac{4\mu(\lambda + \mu)}{\lambda + 2\mu}\Theta_2$$

$$A_4 = \frac{\tilde{Q}\Theta_1}{\tilde{C}\tilde{R} - \tilde{Q}^2} \quad A_5 = \frac{\tilde{C}\Theta_1}{\tilde{C}\tilde{R} - \tilde{Q}^2} \quad A_6 = \frac{\tilde{R}\Theta_1}{\tilde{C}\tilde{R} - \tilde{Q}^2} + \frac{\lambda\Theta_2}{\lambda + 2\mu} \quad A_7 = \frac{\Theta_1}{\tilde{L}} + \frac{\Theta_2}{\mu}$$

(1.4)

$$\Delta = \tilde{P}\tilde{C}\tilde{R} + 2\tilde{F}\tilde{Q}\tilde{M} - \tilde{C}\tilde{M}^2 - \tilde{R}\tilde{F}^2 - \tilde{P}\tilde{Q}^2$$

Impermeable elastic layer is defined by Lame parameters λ, μ and density $\hat{\rho}$. Moduli P, F, M, C, Q, R and L and densities, ρ, ρ_f and mx make up positive definite and symmetric matrices:

$$\begin{pmatrix} R & F & M & 0 \\ F & C & Q & 0 \\ M & Q & R & 0 \\ 0 & 0 & 0 & L \end{pmatrix}, \quad \begin{pmatrix} \rho & \rho_f \\ \rho_f & m_x \end{pmatrix} \qquad (1.5)$$

The effective model described by Equations (1.1) and (1.2) is a special case of the transversely isotropic Biot model where:

$$m_z = \infty \qquad (1.6)$$

From relation (1.6) it follows that in this case conventional equation of the porous medium:

$$-\frac{\partial p}{\partial z} = \rho_f \frac{\partial^2 U_z}{\partial t^2} + m_z \frac{\partial^2 W_z}{\partial t^2} \qquad (1.7)$$

is replaced by relation $W_z = 0$. Physically it means that fluid could not penetrate inside impermeable material of elastic layers. After that number of equations and variables is reduced and is equal to seven.

In order to investigate the effective model it is useful to derive the corresponding Lame's Equation. Substituting Equations (1.1) into (1.2) yields (1.8).

2 CHARACTERISTIC FUNCTIONS $\alpha(\tau)$

For the solution of Equation (1.8) one could obtain integral representation using Fourier integrals. In this case wave field is defined as superposition of plane waves of the form:

$$e^{ik(\tau t - x - \alpha z)} \qquad (2.1)$$

In expression (2.1) we introduce:

$$\tau = v_{ph}/\sin\varphi \quad \alpha = \text{ctg}\varphi \qquad (2.2)$$

where v_{ph} is phase velocity, φ is an angle between the normal to the plane front and the z-axis and k is the component of wave vector along the x-axis. Point source is placed at the origin of coordinates. In order to define the fronts it is sufficiently to calculate the internal integral by the saddle-point method. Saddle points themselves satisfy the equation:

$$t - \alpha'(\tau)\,z = 0 \qquad (2.3)$$

Another relation is condition of singularities of the external integral:

$$\tau t - x - \alpha z = 0 \qquad (2.4)$$

Combining Equations (2.3) and (2.4) yields:

$$x = t\,(\tau - \alpha(\tau)/\alpha'(\tau)), \qquad z = t/\alpha'(\tau) \qquad (2.5)$$

This parametric representation of wave fronts from the point source at the origin was derived by Molotkov and Khilo (1984). It should be noted that only real intervals of parameter τ with real values of function $\alpha(\tau)$ must be used in relations (2.5).

In order to determine the characteristic function $\alpha(\tau)$ it is necessary to replace, according to (2.1), the operation of differentiation by coefficients:

$$\frac{\partial}{\partial x} \sim 1 \qquad \frac{\partial}{\partial z} \sim \alpha \qquad \frac{\partial}{\partial t} \sim -\tau \qquad (2.6)$$

After this replacement the condition of compatibility of the obtained Equation (1.8) is expressed by:

$$\begin{vmatrix} P + L\alpha^2 - \rho\tau^2 & (F+L)\alpha & M - \rho_f\tau^2 \\ (F+L)\alpha & L + C\alpha^2 - \rho\tau^2 & Q\alpha \\ M - \rho_f\tau^2 & Q\alpha & R - m_x\tau^2 \end{vmatrix} = 0 \quad (2.7)$$

Calculation of the determinant yields:

$$A(\tau)\alpha^4 + B(\tau)\alpha^2 + \bar{C}(\tau) = 0 \qquad (2.8)$$

where (2.9).

$$\left(P\frac{\partial^2}{\partial x^2} + L\frac{\partial^2}{\partial z^2} - \rho\frac{\partial^2}{\partial t^2} \right)U_x + (F+L)\frac{\partial^2 U_z}{\partial x \partial z} + \left(M\frac{\partial^2}{\partial x^2} - \rho_f\frac{\partial^2}{\partial t^2} \right)W_x = 0$$

$$(F+L)\frac{\partial^2 U_x}{\partial x \partial z} + \left(L\frac{\partial^2}{\partial x^2} + C\frac{\partial^2}{\partial z^2} - \rho\frac{\partial^2}{\partial t^2} \right)U_z + Q\frac{\partial^2 W_x}{\partial x \partial z} = 0 \qquad (1.8)$$

$$\left(M\frac{\partial^2}{\partial x^2} - \rho_f\frac{\partial^2}{\partial t^2} \right)U_x + Q\frac{\partial^2 U_z}{\partial x \partial z} - \left(R\frac{\partial^2}{\partial x^2} - m_x\frac{\partial^2}{\partial t^2} \right)W_x = 0$$

The solutions of Equation (2.8) are represented by formulas:

$$\alpha_{1,2}^2 = \frac{-B \pm \sqrt{B^2 - 4A\overline{C}}}{2A} \qquad (2.10)$$

In the Equation (2.10) square root is considered as its arithmetical value. The advantage of our approach is that relations (2.5), (2.10), and (2.9) give a possibility to investigate the fronts analytically.

3 CONSTRUCTING THE GRAPHS OF FUNCTIONS $\alpha_{1,2}(\tau)$

In order to construct fronts using Equations (2.5) first it is necessary to build the graphs of functions $\alpha_{1,2}(\tau)$ for all real values τ and α, satisfying Equation (2.8).

It will be shown later on, that these graphs consist of six branches. Let us prove that arbitrary straight line:

$$\alpha = \kappa\tau + \beta \qquad (3.1)$$

could intersect the graphs of functions $\alpha(\tau)$ no more than at six points. Indeed, the abscissa and the ordinate of the points of intersection satisfy the equation, which is obtained by substitution of variables or from (3.1) into Equation (2.8). Resulting equation is of sixth order and it could not have more than six real roots.

Therefore maximum number of intersections is also six. Similar arguments were established while investigating the slowness surfaces (Fedorov, 1968; Musgrave, 1970).

From formulas (2.10) it follows that every real value τ corresponds to at most four real values of α. Therefore an arbitrary straight line τ = const. intersects the graphs of function $\alpha(\tau)$ maximum at four points.

Substituting expression (2.9) into Equation (2.8) we obtain new form of Equation (2.8):

$$F(\tau^2, \alpha^2) = 0 \qquad (3.2)$$

This form shows that the graphs of functions $\alpha(\tau)$ are symmetric with respect to the τ- and α-axes. They also possess the central symmetry with respect to the origin. Due to these properties we could consider only first quadrant $\tau > 0$ and $\alpha > 0$ while constructing the graphs.

We start the investigation of functions $\alpha_{1,2}(\tau)$ from the case $\tau = 0$ which yields (3.3).

For $\tau = 0$ it is easy to check that: $A > 0$, $\overline{C} > 0$, and $\sqrt{B^2 - 4A\overline{C}} < |B|$.

For existence of positive values $\alpha_{1,2}^2(0)$ it is necessary to satisfy additional inequality:

$$2L(RF - QM) > \begin{vmatrix} P & F & M \\ F & C & Q \\ M & Q & R \end{vmatrix} \qquad (3.4)$$

However if this is true, then $B^2 - 4A\overline{C} < 0$ and therefore functions $\alpha_{1,2}^2$ are apparently complex. Thus the values $\alpha_1^2(0)$ and $\alpha_2^2(0)$ are either negative or complex and are not related to the fronts.

$$A(\tau) = L\left(CR - Q^2 - Cm_x\tau^2\right)$$

$$B(\tau) = \tau^4\left(L\rho m_x + C\rho m_x - C\rho_f^2\right) + \tau^2\left[\rho\left(Q^2 - LR - RC\right) + 2\rho_f\left(CM - LQ - FQ\right) + m_x\left(F^2 + 2FL - PC\right)\right]$$
$$+ PCR - PQ^2 - CM^2 - R(F + L)^2 + 2QM(F + L) + RL^2$$

$$\overline{C}(\tau) = \left(L - \rho\tau^2\right)\left[\left(\rho m_x - \rho_f^2\right)\tau^4 - \left(R\rho + Pm_x - 2M\rho_f\right)\tau^2 + PR - M^2\right]$$

(2.9)

$$A + L\left(CR - Q^2\right) \quad \tilde{C} = L\left(PR - M^2\right) \quad B + \begin{vmatrix} P & F & M \\ F & C & Q \\ M & Q & R \end{vmatrix} + 2L(QM - RF)$$

(3.3)

$$B^2 - 4A\overline{C} = \begin{vmatrix} P & F & M \\ F & C & Q \\ M & Q & R \end{vmatrix}\left[\begin{vmatrix} P & F & M \\ F & C & Q \\ M & Q & R \end{vmatrix} + 4L(QM - RF) - 4L^2R\right]$$

In the case of large τ, saving in Equation (2.9) only terms of highest power on yields:

$$\alpha_1 = \tau\sqrt{\frac{\rho m_x - \rho_f^2}{Lm_x}} \qquad \alpha_2 = \tau\sqrt{\frac{\rho}{C}} \qquad (3.5)$$

The Equation (3.5) define the asymptotes of the graphs of functions $\alpha_1^2(\tau)$ and $\alpha_2^2(\tau)$. According to formulas (2.5), graphs near asymptotes (3.5) describe the regions of fronts that are in vicinity of the z-axis. Intersections of fronts with z-axis occur at points:

$$\nu_4 = \sqrt{C/\rho} \qquad \nu_6 = \sqrt{Lm_x/\left(\rho m_x - \rho_f^2\right)} \qquad (3.6)$$

which correspond to infinite values of τ. According to second relation (2.2) these parts of fronts are orthogonal to z-axis because α_1 and α_2 are infinite.

To study the intermediate values of τ we use Viete theorem which yields for production of α_1^2 and α_2^2:

$$\alpha_1^2\alpha_2^2 = \bar{C}(\tau)/A(\tau) \qquad (3.7)$$

Hence $\alpha_1(t)$ or $\alpha_2(t)$ become zero at points (3.8) and become infinite when:

$$v_7^2 = (CR - Q^2)/(m_xC) \qquad (3.9)$$

Points (3.8) and (3.9) divide the half-axis $0 < \tau < \infty$ into 5 intervals. Let us consequently number these intervals from right to left. First interval is determined as $\tau_1 < \tau < \infty$.

According to (2.5), points ($\tau = v_1$, $\alpha = 0$), ($\tau = v_2$, $\alpha = 0$), ($\tau = v_3$, $\alpha = 0$) and ($\tau = v_7$, $\alpha = 0$) define the intersections of fronts with x-axis. By means of (2.2) we find that fronts are orthogonal to the axis at points (3.8) and tangent at point (3.9). Therefore along x-axis there are 4 fronts whereas only 2 fronts are along z-axis. Expressions for v_1, v_2 and v_6 are coincident with that for transversely isotropic Biot model.

Formulas for v_3 and v_4 are obtained from known relations (3.10) for transversely isotropic Biot model by the passage to the limit $m_z \to \infty$. During this passage velocity v_5 vanishes.

Now let us formulate the properties of graphs of $\alpha_{1,2}(\tau)$:
– It is forbidden for them to have extremums because otherwise:

$$\alpha_{1,2}'(\tau) = 0 \qquad (3.11)$$

which means infinite velocity of wave propagation.
– Functions $\alpha_{1,2}(\tau)$ may be both increasing and decreasing. Function $\alpha(\tau)$ changes its sign only through the points where $\alpha' = \infty$.
– Convexity and concavity of fronts are defined by function:

$$\frac{\partial^2 x}{\partial z^2} = \frac{\alpha'(\tau)^3}{t\alpha''(\tau)} \qquad (3.12)$$

which is a consequence of (2.5).
– Cusps of the fronts correspond to the points where $\alpha'(\tau) = 0$ or $\alpha'(\tau) = \infty$.
– Additional intersections with axes (where angle between normal to the front and axis is neither 0 nor 90 degrees) correspond to so called turning points where $\alpha(\tau) \neq 0$ and $\alpha'(\tau) = \infty$.
– If function $\alpha(\tau) = 0$ then, according to (2.10), in this point $\alpha'(\tau) = \infty$.
– In third and fifth intervals there may be subintervals (τ_0, τ_1) where $B^2 - 4A\bar{C} < 0$. In these subintervals $\alpha_1(\tau)$ and $\alpha_2(\tau)$ are complex and therefore they do not define fronts. For constructing the fronts we have to consider only boundary points $\tau = \tau_0$, $\tau = \tau_1$ where

$$\begin{aligned}\alpha_1(\tau_0) = \alpha_2(\tau_0) > 0 \\ \alpha_1(\tau_1) = \alpha_2(\tau_1) > 0\end{aligned} \qquad (3.13)$$

If these conditions are satisfied the we obtain:

$$\begin{aligned}\alpha_1'(\tau_0) = -\alpha_2'(\tau_0) = -\infty \\ \alpha_1'(\tau_1) = -\alpha_2'(\tau_1) = \infty\end{aligned} \qquad (3.14)$$

$$\nu_{1,2}^2 = \frac{R\rho + Pm_x - 2M\rho_f \pm \sqrt{\left(R\rho + Pm_x - 2M\rho_f\right)^2 - 4\left(PR - M^2\right)\left(\rho m_X - \rho_f^2\right)}}{2\left(\rho m_x - \rho_f^2\right)} \qquad \nu_3^2 = L/\rho \qquad (3.8)$$

$$\nu_{4,5}^2 = \frac{R\rho + Cm_z - 2Q\rho_f \pm \sqrt{\left(R\rho + Cm_Z - 2Q\rho_f\right)^2 - 4\left(CR - Q^2\right)\left(\rho m_Z - \rho_f^2\right)}}{2\left(\rho m_x - \rho_f^2\right)} \qquad \nu_3^2 = LM_z/\left(\rho m_z - \rho_f^2\right) \qquad (3.10)$$

On Figure 2 one can see graphs of functions $\alpha_{1,2}$ in the vicinity of points τ_0 and τ_1 when conditions (3.14) hold. We call these points as turning points. If first (second) condition (3.13) is not satisfied then left (right) branch should be absent on (Fig. 2). According to (2.5) and (3.14), point $\tau = \tau_i$ ($i = 1,2$) for $\alpha(\tau_i) > 0$ corresponds to the front point $x = \tau_i t$, $z = 0$. The angle between front and x-axis is defined by value of $\alpha(\tau_i)$.

– Theoretically there is a possibility when graphs $\alpha_1(\tau)$ and $\alpha_2(\tau)$ have one common point of intersection $\tau = \tau_0$. It may happen when the subinterval with negative discriminant reduces to point ($\tau_0 \rightarrow \tau_1$) as it is shown on Figure 3. However this case will not be considered here.

For wave fronts construction we consider three different velocity relations:

$$\begin{array}{lll} \text{I} & v_1 > v_7 > v_{2,3} > v_{3,2} & \\ \text{II} & v_1 > v_{2,3} > v_7 > v_{3,2} & (3.15) \\ \text{III} & v_1 > v_{2,3} > v_{3,2}, v_7 & \end{array}$$

By means of established properties, limiting points and asymptotes we have constructed graphs of $\alpha_{1,2}(\tau)$ for all three cases I, II and III respectively (Fig. 4a, 5a and 6a). Moreover we have made some additional assumptions for these graphs:

– Number of inflection points is taken minimal. Fronts that starts from points ($\tau = v_1$, $\alpha = 0$), ($\tau = v_{2,3}$, $\alpha = 0$) are assumed convex. Triangular front has only one inflection point which on all figures is denoted by bold point.

– We exclude the turning points given on Figure 2. For this purpose we assume that if there is an subinterval (τ_0, τ_1) where $B^2 - 4A\bar{C} < 0$ then $\alpha_1 (\tau_0) = \alpha_2 (\tau_0) < 0$, $\alpha_1 (\tau_1) = \alpha_2 (\tau_1) < 0$.

– Graphs approaching asymptotes $\alpha = \tau/v_4$, $\alpha = \tau/v_6$, and $\tau = v_7$ do not intersect them.

Finally we present the full graph (Fig. 7) of characteristic functions $\alpha(\tau)$ for the case when second inequality (3.14) is satisfied together with the three mentioned conditions about absence of singularities.

4 THE WAVE FRONTS FROM A POINT SOURCE

By means of (2.5) and graphs for $\alpha(\tau)$ we construct a wave fronts from a point source (group velocity curves) in the effective model of alternating porous and solid layers. As before point source is placed at the origin.

Since the fronts are symmetric with respect to x- and z-axes then we draw them only in first quadrant $x > 0$, $z > 0$. Figures 4b, 5b, and 6b correspond respectively to the cases I, II, and III from (3.15). For $\alpha > 0$, $\tau > 0$ most fronts are in the first quadrant however on (Fig. 6b) triangular front is situated in quadrant $x > 0$, $z < 0$. It has a symmetric part in the first quadrant, which is shown by dashed line on (Fig. 6b).

The first outer front is always convex. It may not have any loops because the corresponding branch 1 (Fig. 7) does not have inflection points for arbitrary set
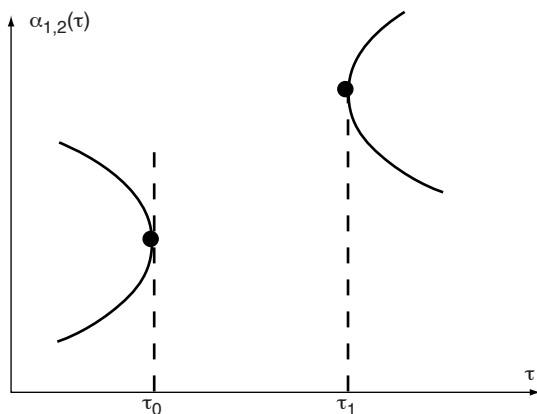

Figure 2

Turning points on graphs of characteristic functions $\alpha_{1,2}(\tau)$.
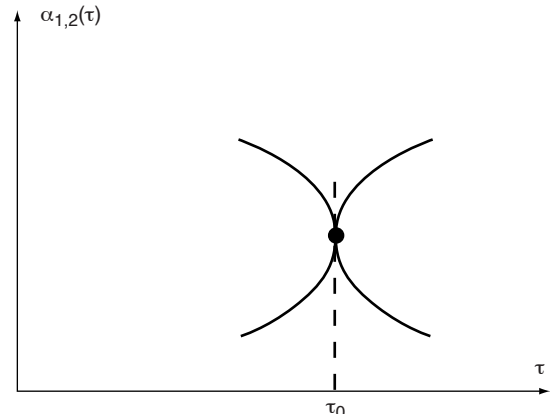

Figure 3

Possible intersection of graphs of characteristic functions $\alpha_{1,2}(\tau)$.

of parameters. Let us prove that for this branch all three assumptions made in Section 3 are correct. Indeed, if we assume that the first branch has two points of inflection then we can find a straight line that intersects the branch 1 three times. This line would also intersect branches 2, 3, 4, and 5 (Fig. 7) and there would be at least 7 intersections. However Christoffel Equation (2.8), which is of 6th order with respect to τ, allows only 6 intersections. Therefore made assumption is incorrect. By the same way one could prove that branch 1 does not intersect its asymptote $\alpha = \tau/v_4$. Turning points are also impossible on branch 1 as otherwise there would be a straight lines $\tau = \text{const.}$, which intersects the branches 1 and 2 at least 6 times. This is not allowed by Equation (2.8), which is of 4th order with respect to α. Hence all three assumptions are correct for the first outer front and it is proved to be convex.

The second branch may have 2 points of inflection (Fig. 8a) which correspond to two cusps of ordinary loop on the second front (Fig. 9a). Theoretically however there is a possibility for existence of double loops on second front (Molotkov and Bakulin, 1996).

If second branch intersects the asymptote $\alpha = \tau/v_6$ and approaches it from the side of larger values of α (Fig. 8b) then the second front acquires a loop along z-axis which enters into the quadrant $x < 0, z > 0$ (Fig. 9b). Point 2 on (Fig. 8b) is inflection point whereas point 1 (where $\alpha'' = \tau\alpha(\tau)$) is not inflection point. Point 1 is situated between point 1′ —intersection of graph with its asymptote and point 1″, where tangent to graph is parallel to the asymptote (Fig. 8b). On the second front point 1 corresponds to the intersection with z-axis whereas point 2 is a cusp point (Fig. 9b). The front is convex between points 1 and 2 and is concave between 2 and $z = v_6 t$. Additional intersection with asymptote is impossible for branch 2 because otherwise there would be a straight line intersecting all graphs more than at 6 points.

In the case of second and third inequalities (3.15) there is a possibility for existence of one inflection point 1 and one turning point 2 (Fig. 8c). The later is similar to the point $\tau = \tau_1$ on Figure 2. Corresponding wave front has a loop along x-axis that enters into the quadrant $x > 0, z < 0$ (Fig. 9c). The front is convex between 1 and 2 and concave between 1 and $x = v_{2,3} t$ (Fig. 9c). Hence second front may have singularities of three mentioned types. Theoretically they may exist simultaneously if the rule on maximum number of intersections is satisfied.

The third branch of graph $\alpha(\tau)$ and corresponding triangular front may have similar singularities. Third branch may also have only one intersection with its asymptote $\tau = v_7$. It is worth to note that third front on Figures 5b and 6b evolves from the ordinary loops (like that on Figures 9a and 9c) when velocity along z-axis vanishes due to $m_z \rightarrow \infty$. Therefore existence of additional turning and inflection points leads to double loops (Molotkov and Bakulin, 1996). Possible turning point positions are shown on Figures 10a, 10b, 10c and 10d. Corresponding wave fronts are given on Figures 11a, 11b, 11c and 11d. All graphs are constructed for effective model (1.1)-(1.2) with the same densities $\rho = 2.36$ g/cm^3, $\rho_f = 1$ g/cm^3, $m_x = 15$ g/cm^3, whereas the elastic moduli are different and given on Table 1.

Cases when there is no turning point but there are 2 inflection points are also possible. It corresponds to double loops on the third front inside the first quadrant (Molotkov and Bakulin, 1996) and is not considered here.

TABLE 1

Elastic moduli for Figures 10 and 11

Case	P, GPa	F, GPa	M, GPa	C, GPa	Q, GPa	R, GPa	L, GPa
Figure 10a	20	4.3	5	25	5	2	3
Figure 10b	33.2	4.3	2.2	25.2	2.2	0.4	5
Figure 10c	20	4.3	5	25	5	2	14
Figure 10d	31.2	4.3	1.1	6	1.1	0.4	30

CONCLUSIONS

Three waves propagate in the effective (long-wave equivalent) model of alternating porous and impermeable solid layers. First wave front is always convex. It corresponds to the first or ordinary longitudinal wave. Second and third fronts correspond to shear and "slow" (second) longitudinal waves or their combination. Second front may have loops between or along axes. Third front is "triangular" and is bounded by some angle whose bisectrix is x-axis.

The "triangular" wave front may have double loops between or along axes. Existence of double loops leads to additional cusps on this wave front.

Developed approach for construction of wave fronts is based on rational choice of characteristic function. Fronts are defined parametrically which affords analytic analysis of such front singularities as cusps or
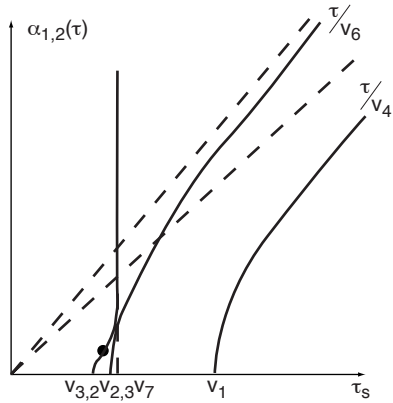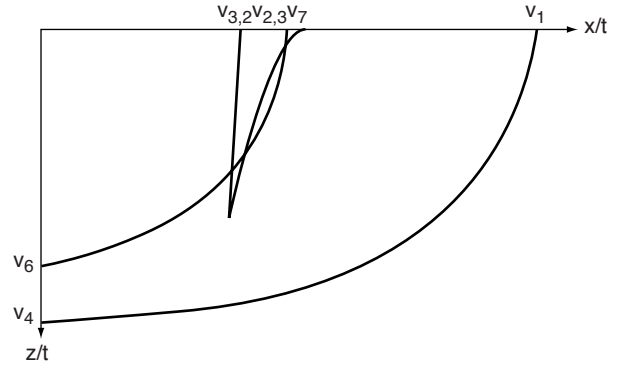
Figure 4a

Figure 4b

Graphs of characteristic functions $\alpha_{1,2}(\tau)$ (a) and corresponding wave fronts (b) for case I (see (3.15)).
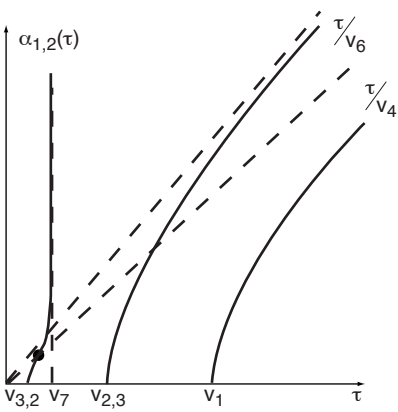
Figure 5a

Figure 5b

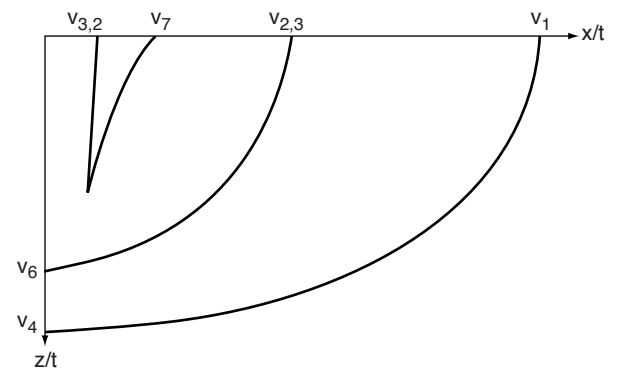Same as Figure 4 for case II (see (3.15)).
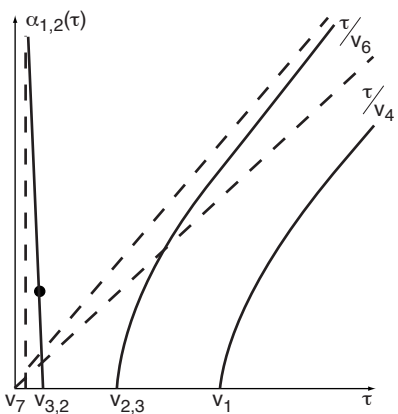
Same as Figure 4 for case II (see (3.15)).

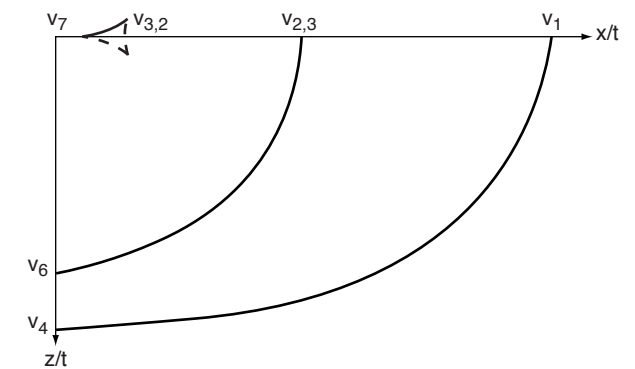Figure 6a

Figure 6b

Same as Figure 4 for case III (see (3.15)).
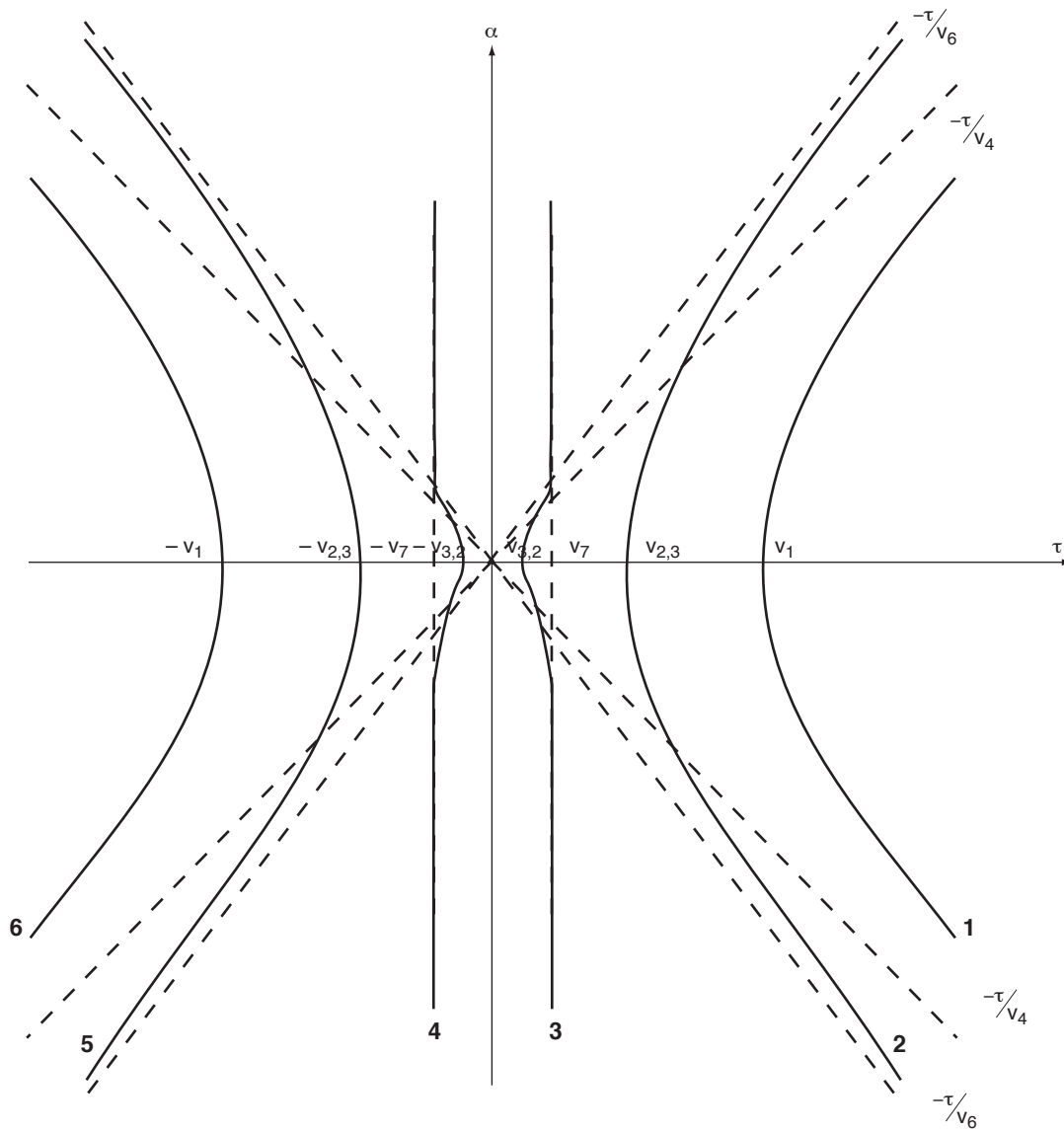
Same as Figure 4 for case III (see (3.15)).

Figure 7

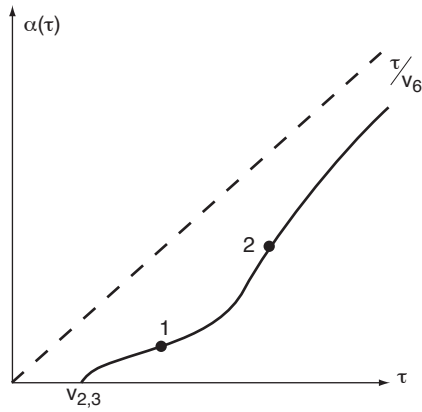Graphs of characteristic functions $\alpha_{1,2}(\tau)$ in all quadrants with asymptotes.

Figure 8a

Characteristic function $\alpha(\tau)$ for different location of loop: loop between axes. Corresponding fronts are shown on Figure 9a.
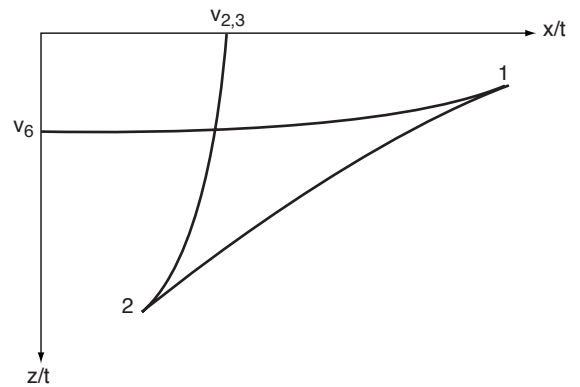
Figure 9a

Wase fronts corresponding to characteristic functions $\alpha(\tau)$ shown on Figure 8a.
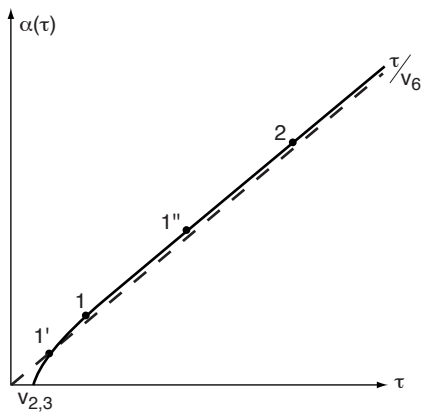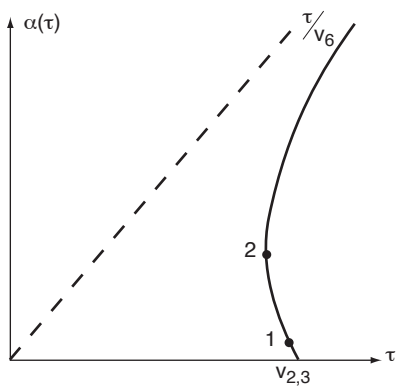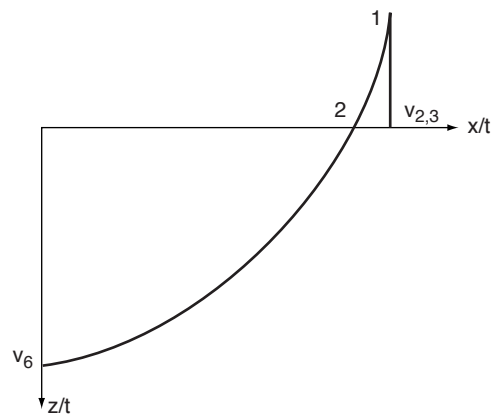

Figure 8b

Characteristic function $\alpha(\tau)$ for different location of loop: loop on z-axis. Corresponding fronts are shown on Figure 9b.
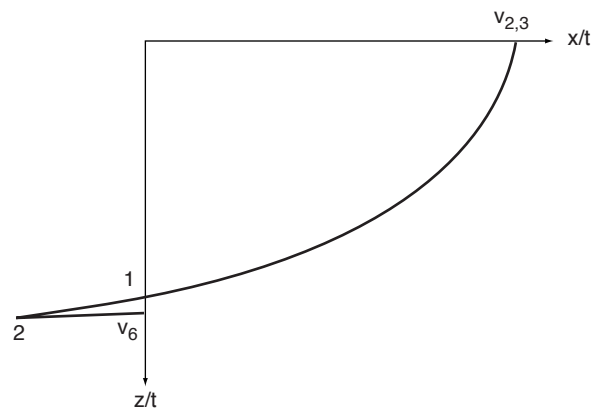
Figure 9b

Wase fronts corresponding to characteristic functions $\alpha(\tau)$ shown on Figure 8b.

Figure 8c

Characteristic function $\alpha(\tau)$ for different location of loop: loop on x-axis. Corresponding fronts are shown on Figure 9c.

Figure 9c

Wase fronts corresponding to characteristic functions $\alpha(\tau)$ shown on Figure 8c.
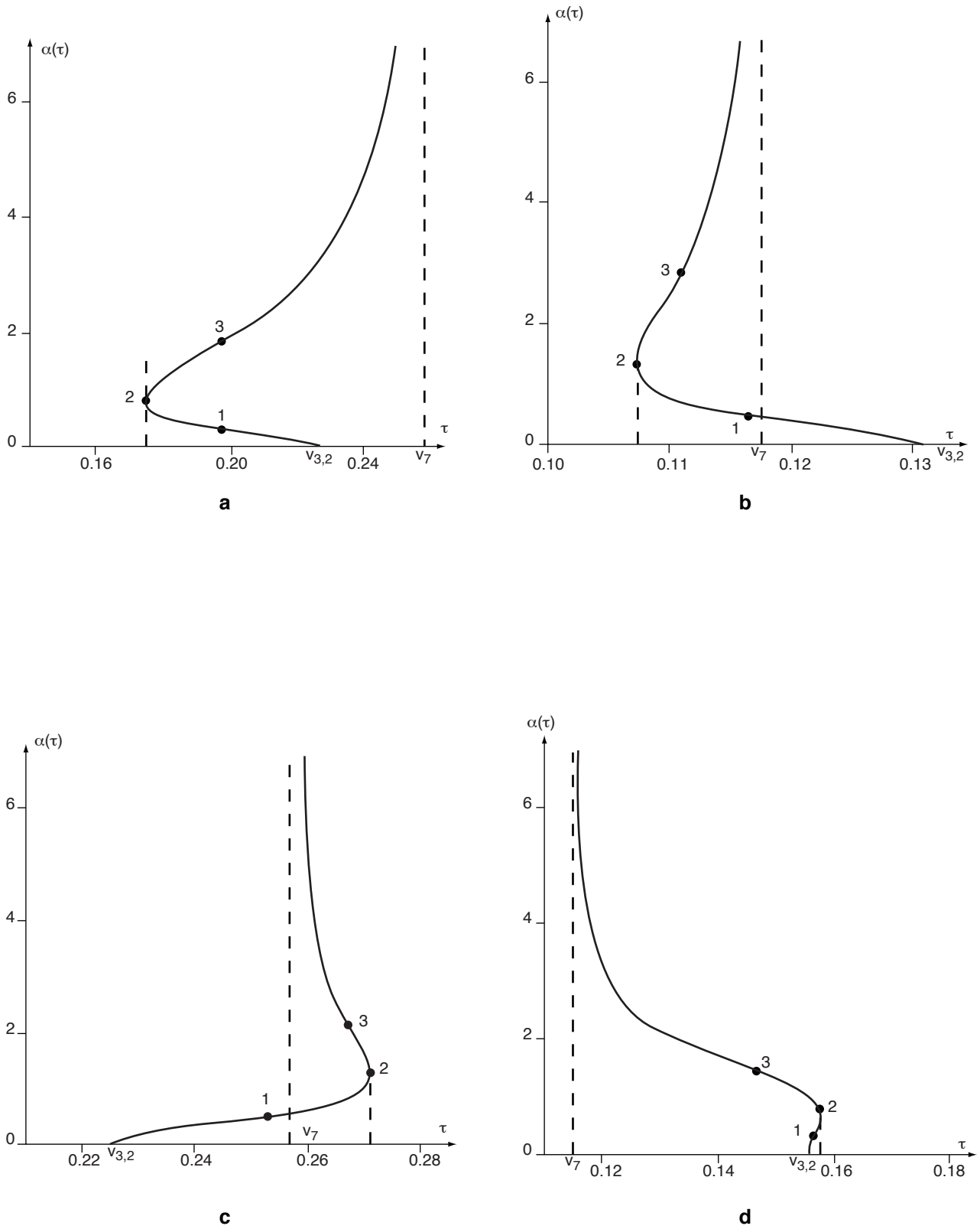
Figure 10

Characteristic functions $\alpha(\tau)$ for different cases of double loops on "triangular" wave front.
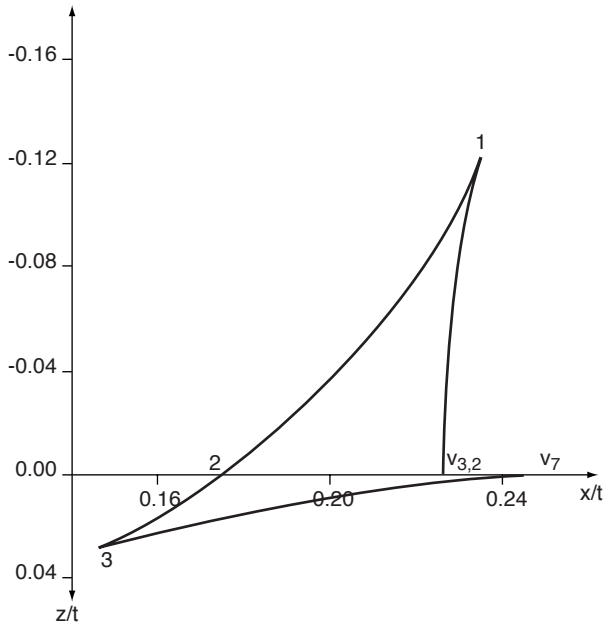
Figure 11a

Different cases of double loops on "triangular" wave front corresponding to characteristic functions $\alpha(\tau)$ of Figure 10a.
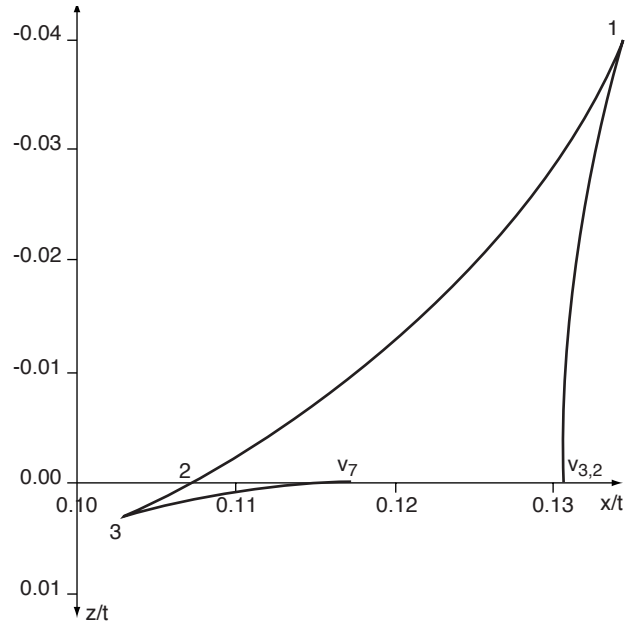
Figure 11b

Different cases of double loops on "triangular" wave front corresponding to characteristic functions $\alpha(\tau)$ of Figure 10b.
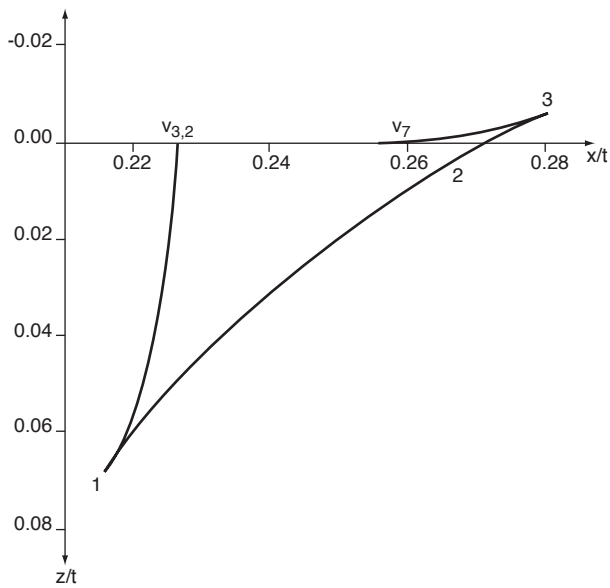
Figure 11c

Different cases of double loops on "triangular" wave front corresponding to characteristic functions $\alpha(\tau)$ of Figure 10c.
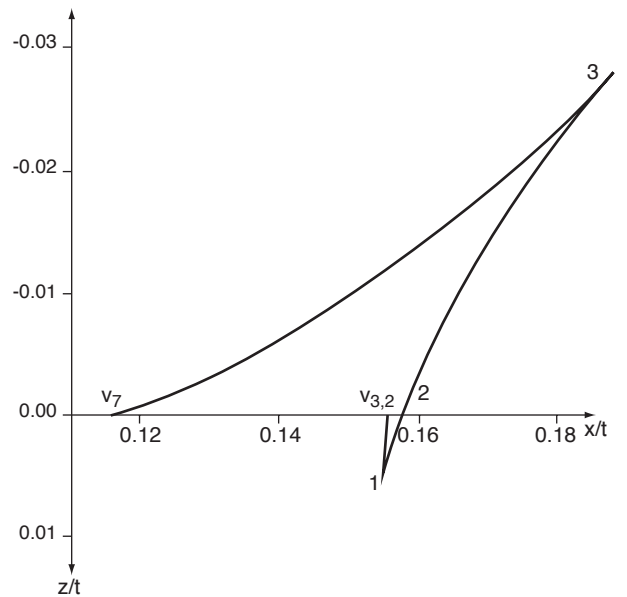
Figure 11d

Different cases of double loops on "triangular" wave front corresponding to characteristic functions $\alpha(\tau)$ of Figure 10d.

intersections with axes. This approach is applicable for broad class of media.

Resulting attenuation in the effective model corresponds to Biot mechanism and does not contain relaxation kernels, which appear in porous-porous model.

As the fronts are defined by terms of highest power on frequency then the term describing viscous dissipation does not affect the wave fronts.

This work is supported by *Russian Fund of Basic Research* under grants N 96-01-00666 and 96-05-66207.

REFERENCES

Bakulin A.V. and Molotkov L.A. (1998) Effective models of thinly-stratified media containing porous, elastic and fluid layers. In: *Amplitude-Preserving Seismic Reflection Imaging, Seismic Application Series*, 2, edited by P. Hubral, Geophysical Press.

Bakulin A.V. and Molotkov L.A. (1997) Generalized anisotropic Biot model as effective model of stratified poroelastic medium. *59th EAGE Conference and Technical Exhibition: Extended Abstracts*, Paper P056, Geneva, Switzerland.

Fedorov F.I. (1968) *Theory of Elastic Waves in Crystals*, Plenum Press.

Helbig K. (1994) Foundations of anisotropy for exploration seismics. Handbook of geophysical exploration. Section I. *Seismic Exploration*, 22. Pergamon.

Hsu C.J. and Schoenberg M. (1993) Elastic wave through a simulated fractured medium. *Geophysics*, 58, 964-977.

Molotkov L.A. and Bakulin A.V. (1997a) The effective models of the stratified media containing porous Biot layers. *Proc. St. Petersburg Branch of Steklov Math. Inst.*, 239, 26, 140-163 (in Russian, to be translated in *J. Math. Sc.* (USA)).

Molotkov L.A. and Bakulin A.V. (1997) Biot description of thinly layered porous medium with impermeable solid layers. *59th EAGE Conference and Technical Exhibition: Extended Abstracts*, Paper P055, Geneva, Switzerland. Paper P055.

Molotkov L.A. and Bakulin A.V. (1996) About the relation between the effective model of layered fluid-solid medium and transversely isotropic Biot model. *58th EAGE Conference and Technical Exhibition: Extended Abstracts*, Paper C013, Amsterdam, The Netherlands, 1.

Molotkov L.A. and Khilo A.E. (1984) Investigation of monophase and multiphase effective models describing periodic systems. *J. Sov. Math.*, 1986, 32, 2.

Musgrave M.J.P. (1970) *Crystal acoustics*, Holden-Day.

Schoenberg M. (1996) Effective medium theory for fractured media in context of Biot theory. *SEG\EAGE Summer Research Workshop "Wave propagation in rocks"*, Big Sky, Montana.

Final manuscript received in July 1998